Research Square

Preprints are preliminary reports that have not undergone peer review.
They should not be considered conclusive, used to inform clinical practice,
or referenced by the media as validated information.

Facile Synthesis and Electrochemical Performance of $CoFe_2O_4$@GO Nanocomposites for Supercapacitor Applications

Rajesh Bhardwaj

rbhardwaj0305@gmail.com

Lovely Professional University

Amit Kumar Atri

Cluster University of Jammu

Anoop Singh

Govt. College for Women (Autonomous)

Aman Deep Acharya

Lovely Professional University

Sandeep Manhas

Lovely Professional University

Research Article

Keywords: Cobalt ferrite, Graphene oxide nanocomposites, Supercapacitors, Electrochemical energy storage, Co-precipitation synthesis

Posted Date: October 28th, 2026

DOI: https://doi.org/10.21203/rs.3.rs-11249003/v1

License: This work is licensed under a Creative Commons Attribution 4.0 International License.
Read Full License

Additional Declarations: No competing interests reported.

Facile Synthesis and Electrochemical Performance of $CoFe_2O_4$@GO Nanocomposites for Supercapacitor Applications

Rajesh Bhardwaj[1,2,#], Amit Kumar Atri[3], Anoop Singh[4], Aman Deep Acharya[1], Sandeep Manhas[1]

[1]School of Chemical Engineering & Physical Sciences, Lovely Professional University Phagwara Jalandhar, Punjab, 144401, India

[2]Department of Physics, G.G.M. Science College (A Constituent College of Cluster University of Jammu), Jammu, Jammu and Kashmir, 180002, India

[3]Department of Chemistry, University of Jammu, Jammu, Jammu and Kashmir, 180006, India

[4]Department of Physics, Higher Education Department, Govt. College for Women (Autonomous), Parade Ground, Jammu, Jammu and Kashmir 180001, India

[#]Corresponding author: rbhardwaj0305@gmail.com

Abstract

In this work, $CoFe_2O_4$ nanoparticles and $CoFe_2O_4$@GO nanocomposites were successfully synthesized using a simple and cost-effective co-precipitation method for potential supercapacitor applications. The incorporation of graphene oxide (GO) into cobalt ferrite was aimed at improving the electrical conductivity and electrochemical performance of the electrode material. The structural, morphological, and chemical properties of the synthesized materials were systematically characterized using X-ray diffraction (XRD), field emission scanning electron microscopy (FESEM), Fourier transform infrared spectroscopy (FTIR), and X-ray photoelectron spectroscopy (XPS). The characterization results confirmed the successful formation of the spinel structured $CoFe_2O_4$ and the effective integration of graphene oxide in the nanocomposite. The electrochemical performance of the prepared materials was investigated using cyclic voltammetry (CV), galvanostatic charge–discharge (GCD), and electrochemical impedance spectroscopy (EIS). The CV curves revealed prominent redox peaks, indicating pseudocapacitive behavior of the electrode materials. The $CoFe_2O_4$@GO nanocomposite exhibited superior electrochemical performance compared to pure $CoFe_2O_4$, which can be attributed to the enhanced electrical conductivity and large surface area provided by graphene oxide. The GCD results demonstrated improved charge storage capability and good rate performance, while the EIS analysis indicated reduced charge transfer resistance in the nanocomposite electrode. Furthermore, the $CoFe_2O_4$@GO electrode showed excellent cyclic stability during repeated charge–discharge cycles. The enhanced electrochemical performance of the $CoFe_2O_4$@GO nanocomposite suggests that it is a promising candidate for high-performance supercapacitor applications.

Keywords: Cobalt ferrite, Graphene oxide nanocomposites, Supercapacitors, Electrochemical energy storage, Co-precipitation synthesis

Introduction

The rapid growth of modern technology and increasing global energy demand have intensified the need for efficient and sustainable energy storage systems [1-3]. Conventional energy sources such as fossil fuels are associated with environmental concerns and limited availability, which has driven extensive research toward alternative and renewable energy technologies [4-6]. Among various energy storage devices, supercapacitors have attracted significant attention due to their high power density, fast charge–discharge capability, long cycle life, and excellent operational stability [7-10]. These unique properties make supercapacitors highly suitable for applications in portable electronics, hybrid electric vehicles, and large-scale energy storage systems [11]. Supercapacitors are generally classified into two main categories: electric double-layer capacitors (EDLCs) and pseudocapacitors. EDLCs store energy through electrostatic charge accumulation at the electrode–electrolyte interface, typically using carbon-based materials such as activated carbon, carbon nanotubes, and graphene [12]. In contrast, pseudocapacitors store energy through fast and reversible faradaic redox reactions occurring at the surface of electrode materials, often involving transition metal oxides, hydroxides, or conducting polymers [13-15]. Among these materials, transition metal oxides have gained considerable attention because of their high theoretical capacitance, multiple oxidation states, and rich electrochemical activity [16,17].

Among the various transition metal oxides, cobalt ferrite ($CoFe_2O_4$) has emerged as a promising electrode material for electrochemical energy storage applications [18-20]. Cobalt ferrite is a spinel-type ferrite with excellent chemical stability, good electrical conductivity, high mechanical strength, and remarkable electrochemical activity arising from the multiple valence states of cobalt and iron ions. These properties enable cobalt ferrite to exhibit efficient faradaic redox reactions during electrochemical processes, making it a suitable candidate for supercapacitor electrodes [21]. Furthermore, cobalt ferrite nanoparticles possess high surface area and structural stability, which contribute to improved electrochemical performance. Despite these advantages, pure cobalt ferrite often suffers from certain limitations such as relatively low electrical conductivity and aggregation of nanoparticles during synthesis [22-24]. These issues can hinder ion diffusion and electron transport within the electrode material, thereby limiting the overall electrochemical performance. To overcome these challenges, researchers have explored the development of nanocomposite materials by integrating cobalt ferrite with conductive carbon-based materials. Among

various carbon materials, GO has attracted significant interest due to its exceptional structural and electronic properties [25-28]. Graphene oxide possesses a two-dimensional layered structure with a large specific surface area and abundant oxygen-containing functional groups such as hydroxyl, epoxy, and carboxyl groups. These functional groups facilitate strong interaction with metal oxide nanoparticles and promote uniform dispersion of the active material on the graphene oxide sheets. Moreover, GO provides an interconnected conductive network that enhances electron transport and improves the overall electrochemical performance of the composite material [29,30]. The incorporation of graphene oxide with cobalt ferrite can lead to a synergistic effect, where cobalt ferrite contributes high pseudocapacitance through redox reactions, while graphene oxide enhances electrical conductivity, surface area, and structural stability. This combination effectively improves charge transfer kinetics, electrolyte ion diffusion, and cycling stability of the electrode material. As a result, $CoFe_2O_4$@GO nanocomposites have emerged as promising candidates for high-performance supercapacitor electrodes.

Various synthesis techniques have been reported for the preparation of cobalt ferrite-based nanostructures, including hydrothermal synthesis, sol–gel methods, thermal decomposition, and co-precipitation methods [31-33]. Among these approaches, the co-precipitation method is widely used due to its simplicity, cost-effectiveness, and ability to produce uniform nanoparticles with controlled composition [34,35]. Additionally, this method allows the easy incorporation of graphene oxide into the ferrite matrix, facilitating the formation of well-dispersed nanocomposites. In the present work, $CoFe_2O_4$ nanoparticles and $CoFe_2O_4$@GO nanocomposites were synthesized using the co-precipitation method. The structural, morphological, and chemical properties of the synthesized materials were characterized using XRD, FESEM, FTIR and XPS. Furthermore, the electrochemical performance of the synthesized materials was investigated using CV, GCD and EIS techniques. The primary objective of this study is to investigate the influence of graphene oxide incorporation on the electrochemical behavior of cobalt ferrite and to evaluate the potential of $CoFe_2O_4$@GO nanocomposites as efficient electrode materials for supercapacitor applications. The results demonstrate that the introduction of graphene oxide significantly enhances the electrochemical performance by improving electrical conductivity, ion diffusion, and charge storage capability. Therefore, the synthesized $CoFe_2O_4$@GO nanocomposite shows promising potential for future high-performance energy storage devices.

Methodology

$CoFe_2O_4$ nanoparticles were synthesized using the co-precipitation method. Analytical grade cobalt nitrate hexahydrate ($Co(NO_3)_2 \cdot 6H_2O$), GO and ferric nitrate nonahydrate ($Fe(NO_3)_3 \cdot 9H_2O$) were used as precursor materials, and deionized (DI) water was used as the solvent. In first step, 2.91 g of cobalt nitrate hexahydrate was dissolved in 100 mL of deionized water to prepare the cobalt precursor solution. Separately, 8.08 g of ferric nitrate nonahydrate was dissolved in 100 mL of DI water and added to the same beaker containing the cobalt solution to maintain the stoichiometric ratio required for $CoFe_2O_4$ formation. The mixed solution was continuously stirred using a magnetic stirrer for 1 hour to ensure complete dissolution and homogeneous mixing of the metal ions. After obtaining a uniform solution, 10 M NaOH solution was added dropwise under constant stirring until the formation of a precipitate was observed. The addition of NaOH facilitated the co-precipitation of cobalt and iron hydroxides. The resulting precipitate was then subjected to heating at 120 °C to promote the formation of cobalt ferrite nanoparticles (**Figure 1**).

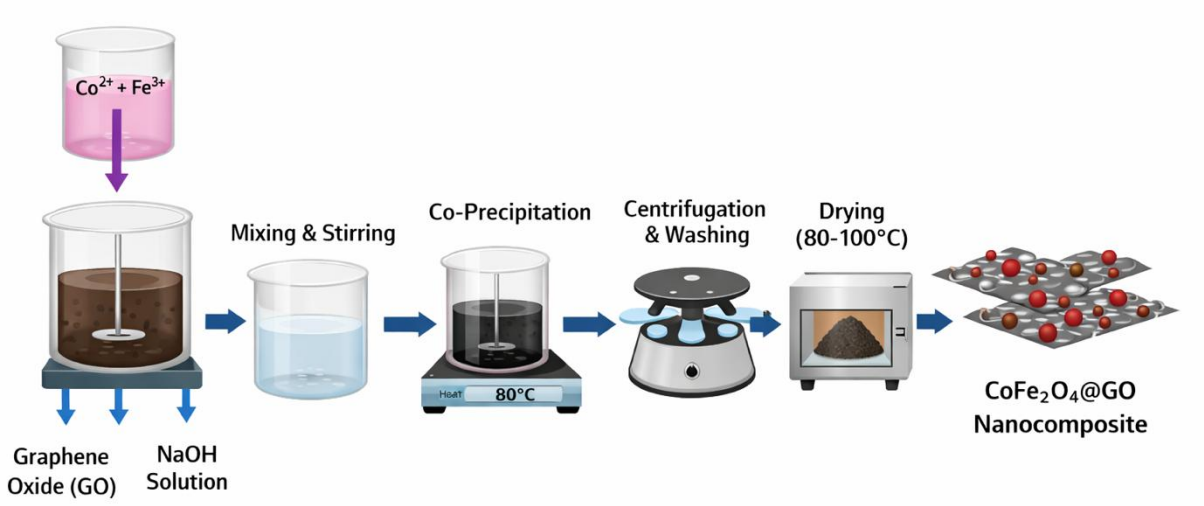


Figure 1: Synthesis steps of $CoFe_2O_4$@GO nanocomposites.

Subsequently, 0.01 g of GO was added to the mixed metal salt solution of $Co(NO_3)_2 \cdot 6H_2O$ and $Fe(NO_3)_3 \cdot 9H_2O$. The resulting suspension was stirred continuously to ensure uniform dispersion of GO sheets within the solution. After achieving a homogeneous mixture, 10 M NaOH solution was added dropwise under constant stirring until the formation of a precipitate was observed, indicating the co-precipitation of cobalt and iron hydroxides in the presence of graphene oxide. The obtained precipitate was then subjected to heat treatment at

120 °C, facilitating the formation of $CoFe_2O_4$ nanoparticles anchored onto graphene oxide sheets, resulting in the formation of $CoFe_2O_4$@GO nanocomposites. The synthesized nanocomposite material was subsequently collected for further characterization.

Characterization Section

The structural, morphological, chemical, and surface properties of the synthesized $CoFe_2O_4$@GO nanocomposites were investigated using various characterization techniques. The crystalline structure and phase purity of the synthesized samples were examined using X-ray diffraction analysis. The surface morphology and microstructural features of the synthesized nanocomposites were studied using FESEM. The surface chemical composition and oxidation states of the elements present in the nanocomposite were analyzed using XPS. Furthermore, FTIR spectroscopy was employed over a suitable wavenumber range to detect the characteristic vibrational bands associated with metal-oxygen bonds and oxygen-containing functional groups of GO.

XRD characterization

The phase and structural identification of the prepared $CoFe_2O_4$ and $CoFe_2O_4$@GO nanocomposites was obtained from XRD as shown in **Figure 2**. The results of XRD pattern reveal that the synthesized $CoFe_2O_4$ nanocomposites show cubic spinel crystal structure with the space group of Fd-3m. All the mentioned peaks can be referred to pure cubic phase structure of $CoFe_2O_4$ specimens (JCPDS number 22-1086) [36]. No other additional peaks were identified in the powder XRD pattern of $CoFe_2O_4$. The peaks at 30.22, 35.34°, 37.96°, 43.27°, 57.41°, 63.69°, correspond to (220), (311), (222), (400), (511), (440) indicating the presence of crystalline $CoFe_2O_4$. The small shift and change in intensity are observed in peaks of $CoFe_2O_4$@GO nanocomposites which confirms the successful incorporation of graphene oxide. The absence of impurity related peaks confirms the high purity and crystallinity of sample.

The average crystallite size of synthesized $CoFe_2O_4$ and $CoFe_2O_4$@GO was calculated using Debye Scherrer formula is given in **equation 1** [37], from the prominent diffraction peaks,

$$D = \frac{K\lambda}{\beta Cos\theta} \qquad (1)$$

where K is equal to 0.9 which is a constant value, λ is the x-ray wavelength, β is the full width at half-maximum (FWHM), and θ denotes the diffraction angle. The average crystallite size of both $CoFe_2O_4$ and $CoFe_2O_4$@GO are found to be 22.44 nm and 19.56 nm respectively.

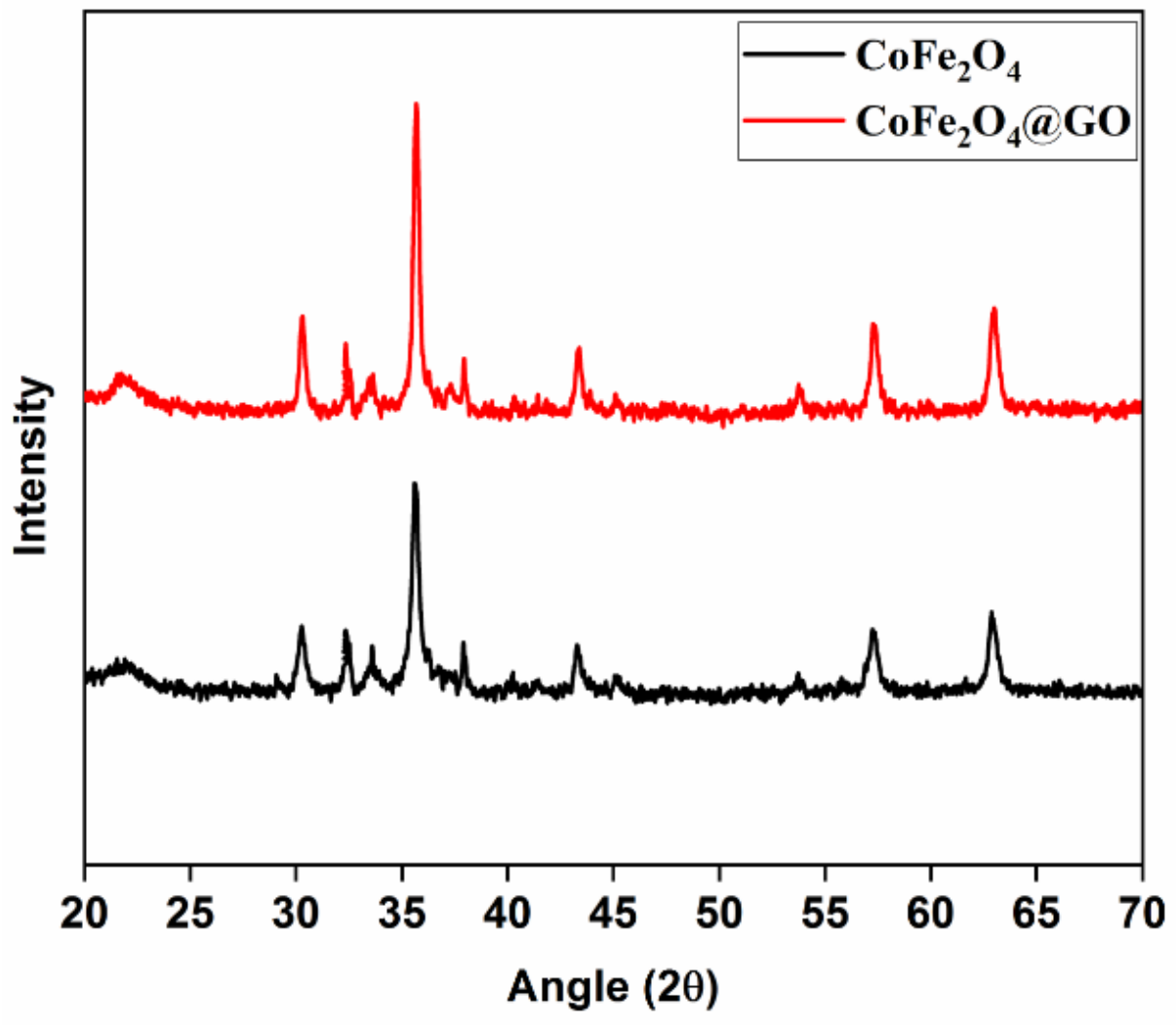


Figure 2: XRD spectra of $CoFe_2O_4$ and $CoFe_2O_4$@GO.

FTIR characterization

Fourier Transform Infrared (FTIR) spectroscopy was used to identify the functional groups and confirm the formation of $CoFe_2O_4$ and $CoFe_2O_4$@GO nanocomposites. The FTIR spectra were recorded over a suitable wavenumber range to analyze the characteristic vibrational bands of the synthesized materials (**Figure 3**). For $CoFe_2O_4$ nanoparticles, the FTIR spectrum exhibited two prominent absorption bands in the low wavenumber region, which are characteristic of the spinel ferrite structure. The band observed around 580–600 cm^{-1}

corresponds to the stretching vibration of metal–oxygen (M–O) bonds at the tetrahedral sites, while the band near 400–450 cm^{-1} is attributed to the metal–oxygen vibrations at the octahedral sites of the spinel lattice [38-40]. These bands confirm the successful formation of cobalt ferrite. In the case of the $CoFe_2O_4$@GO nanocomposite, in addition to the characteristic ferrite bands, several absorption peaks related to graphene oxide (GO) were observed. The broad absorption band around 3400 cm^{-1} corresponds to the stretching vibration of –OH groups, indicating the presence of hydroxyl functional groups [41]. The peak near 1720 cm^{-1} is attributed to the C=O stretching vibration of carboxyl groups, while the band around ~1620 cm^{-1} corresponds to C=C skeletal vibrations of the graphene structure [42]. Additionally, peaks around 1050–1220 cm^{-1} are associated with C–O stretching vibrations of epoxy and alkoxy groups present in GO [43]. The presence of both the characteristic metal–oxygen vibrations of $CoFe_2O_4$ and the oxygen-containing functional groups of GO in the FTIR spectrum confirms the successful formation of the $CoFe_2O_4$@GO nanocomposite. The interaction between cobalt ferrite nanoparticles and graphene oxide sheets further indicates the effective incorporation of GO within the nanocomposite structure.

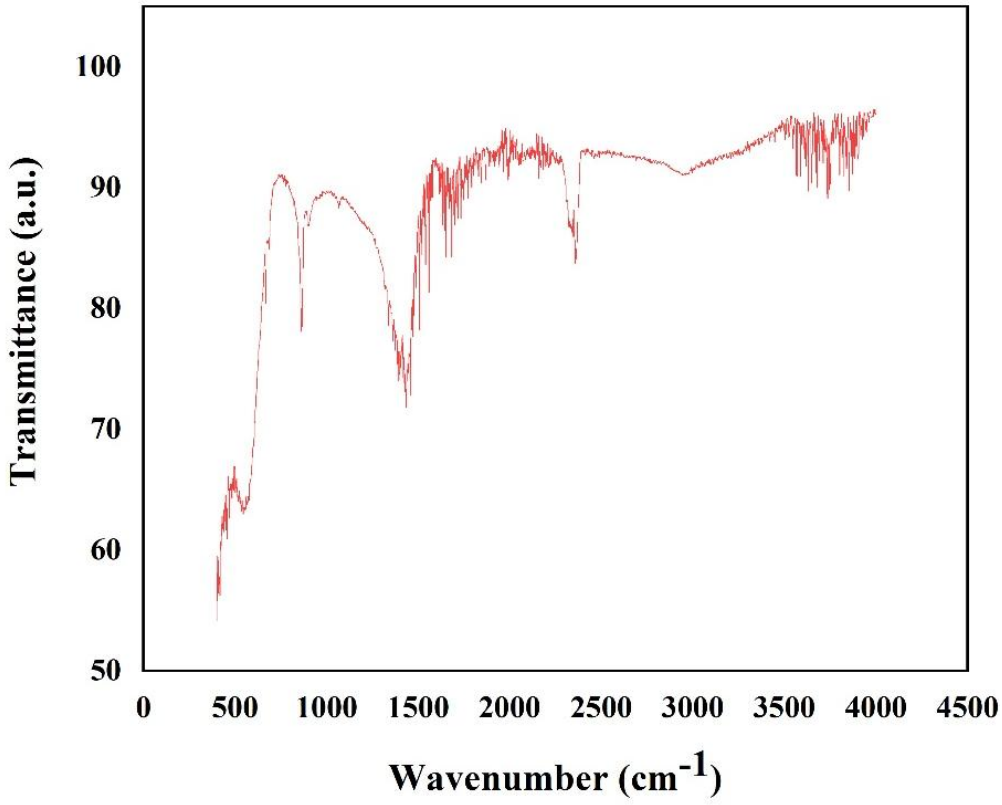


Figure 3: FTIR spectra of $CoFe_2O_4$ and $CoFe_2O_4$@GO.

FESEM characterization

FE-SEM is a versatile technique employed to elucidate the structural and morphological attributes of diverse materials. **Figure 4** shows that smaller $CoFe_2O_4$ clusters tightly deposited on the GO sheets indicating that GO may interact with $CoFe_2O_4$ nanoparticles and inhibit their aggregation. The nanoparticles may interact with graphene sheets through physisorption, electrostatic binding, or charge transfer interaction and the exact mechanism is still under investigation. Because the electrical conductivity of the $CoFe_2O_4$ is low, the well-dispersed GO connected with $CoFe_2O_4$ cluster would form a two-dimensional network for electronic transmission, which would greatly improve the connectivity of $CoFe_2O_4$ particles and the electrical conductivity of the composite.

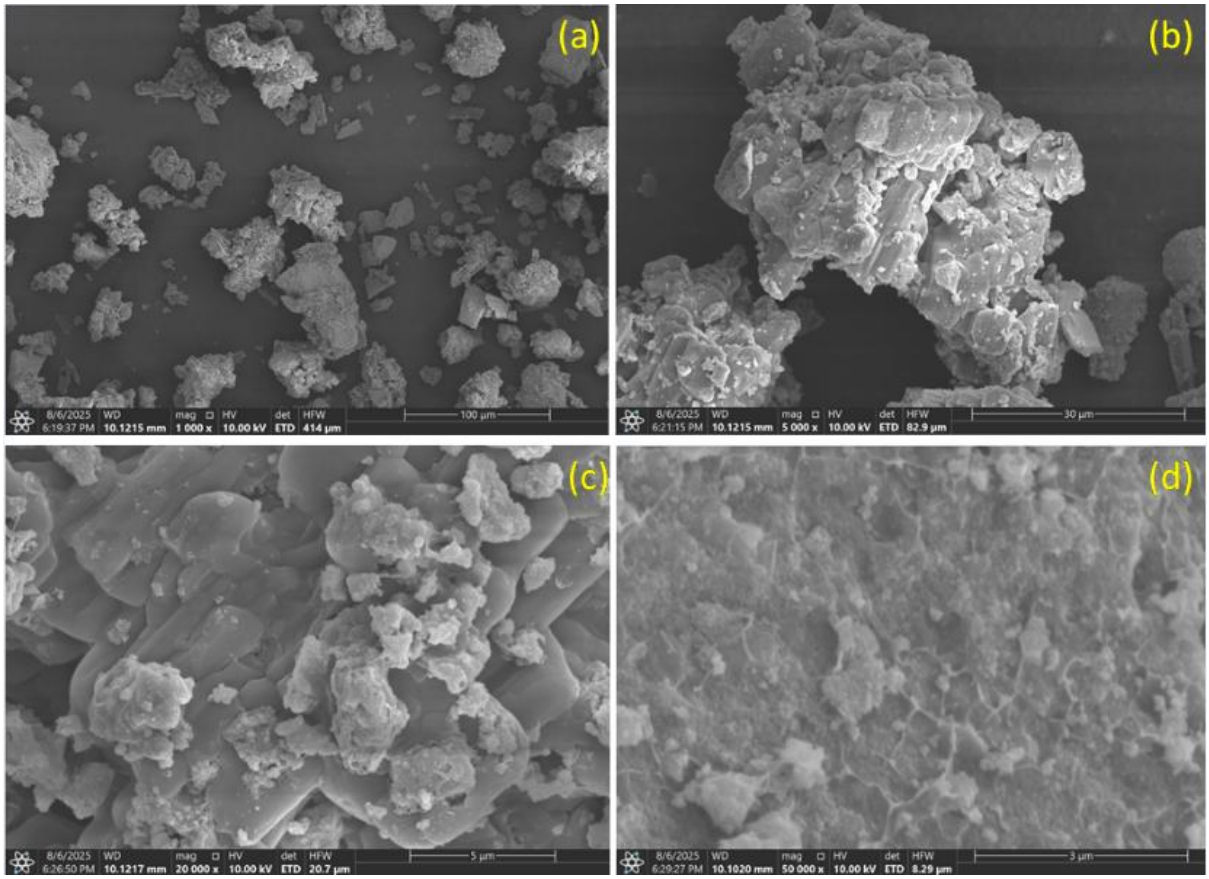


Figure 4: FESEM images $CoFe_2O_4$@GO.

Elemental mapping and EDS characterization

EDS is a microanalytical technique that determines the elemental composition of a sample by measuring the energy and intensity of emitted X-rays. **Figure 5(a)** displays the area scanned for the EDS analysis and elemental mapping. The elemental distribution of Co, Fe, O and C observed through elemental mapping in **Figure 5**(c), (d), (e) and (f) further corroborates the EDS results, as the mapping exclusively highlights the presence of Co, Fe, O and C. The EDS analysis presented in **Figure 6** demonstrates distinct peaks corresponding to Co, Fe, O and C verifying the successful synthesis of $CoFe_2O_4$@GO nanocomposite. According to the EDS results, the atomic percentages (at.%) of Co, Fe, O and C are calculated to be 12.3%, 23.1%, 46.7% and 17.19%, respectively, while the weight percentages (wt.%) are determined to be 24.3% for Co, 43.4 for Fe, 25.1% for O and 7.2% for C.

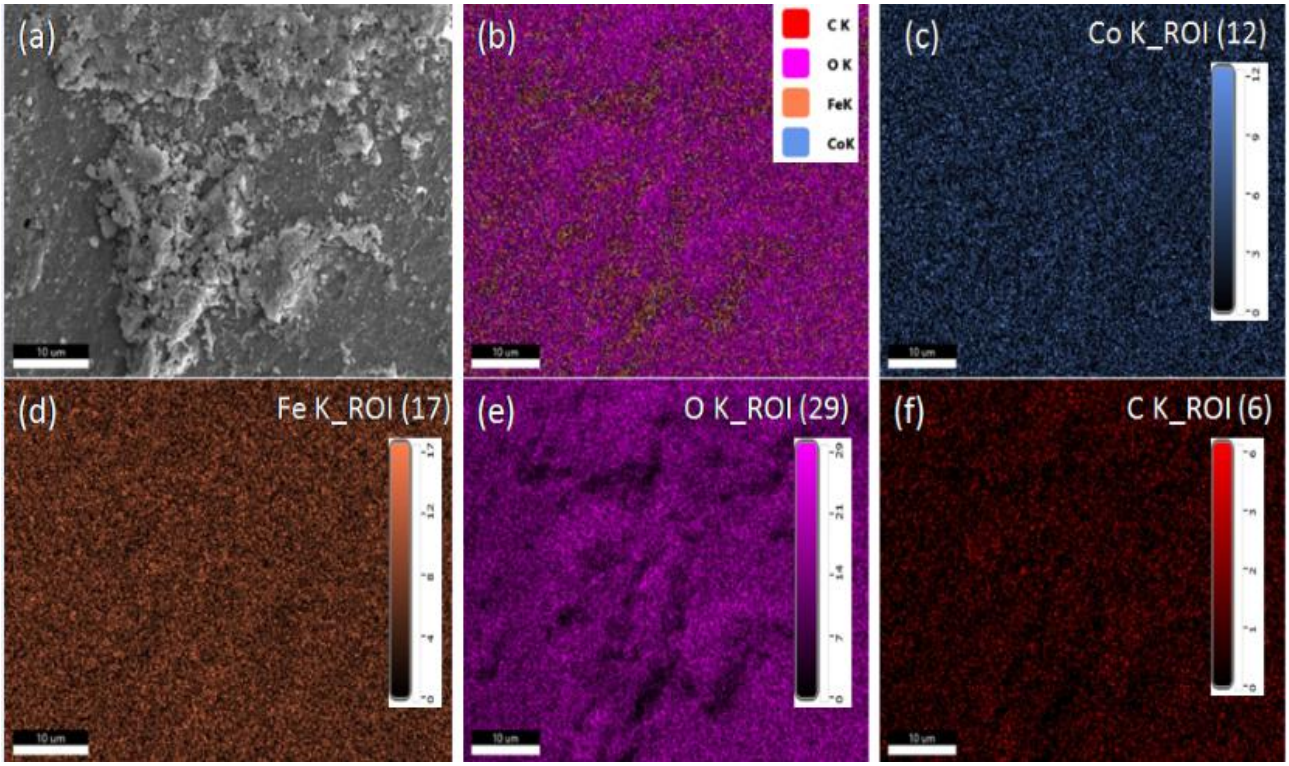
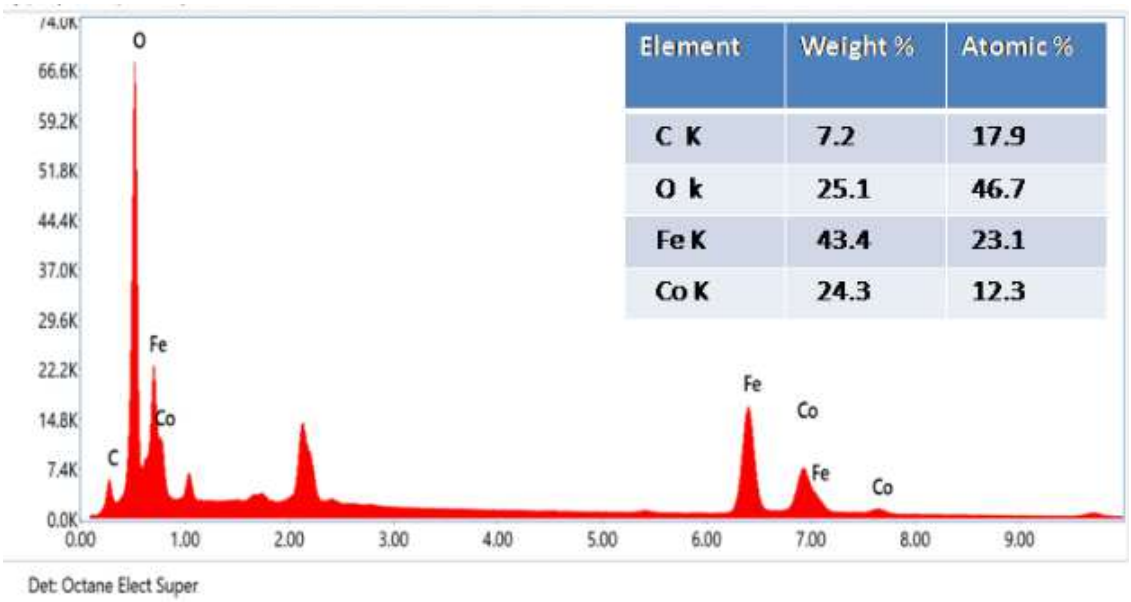


Figure 5: Elemental mapping of $CoFe_2O_4$@GO.



Element	Weight %	Atomic %
C K	7.2	17.9
O k	25.1	46.7
Fe K	43.4	23.1
Co K	24.3	12.3

Figure 6: EDS spectra of $CoFe_2O_4$@GO.

X-ray photoelectron spectroscopy characterization

Chemical composition and chemical state of a material can be qualitatively and quantitatively analyzed using X-ray photoelectron spectroscopy (XPS) [44]. **Figure 7(a)** shows the surface composition analysis of the $CoFe_2O_4$@GO nanocomposite sample that reveals the presence of Co, Fe, O and C elements. Purity of the prepared material can be justified from the survey spectrum. Detailed information on the element's oxidation state was obtained from the high-resolution spectrum of Co 2p shown in **Figure 7(b)** Co 2p spectrum exhibits two major peaks of binding energy 780.11 and 795.49 eV corresponding to Co $2p_{3/2}$ and Co $2p_{1/2}$ respectively [45,46]. **Figure 7(c)** Fe 2p spectrum exhibits two major peaks corresponding to Fe $2p_{3/2}$ and Fe $2p_{1/2}$ respectively. The soft oxidation of graphene was further proved by XPS **Figure 7(d)** [47]. **Figure 7(e)** shows the O 1 s XPS spectrum, which exhibits main peaks at 531 eV. These correspond to surface-adsorbed oxygen species, which are active sites for catalytic reactions, and lattice oxygen, which maintains the integrity of the crystal framework.

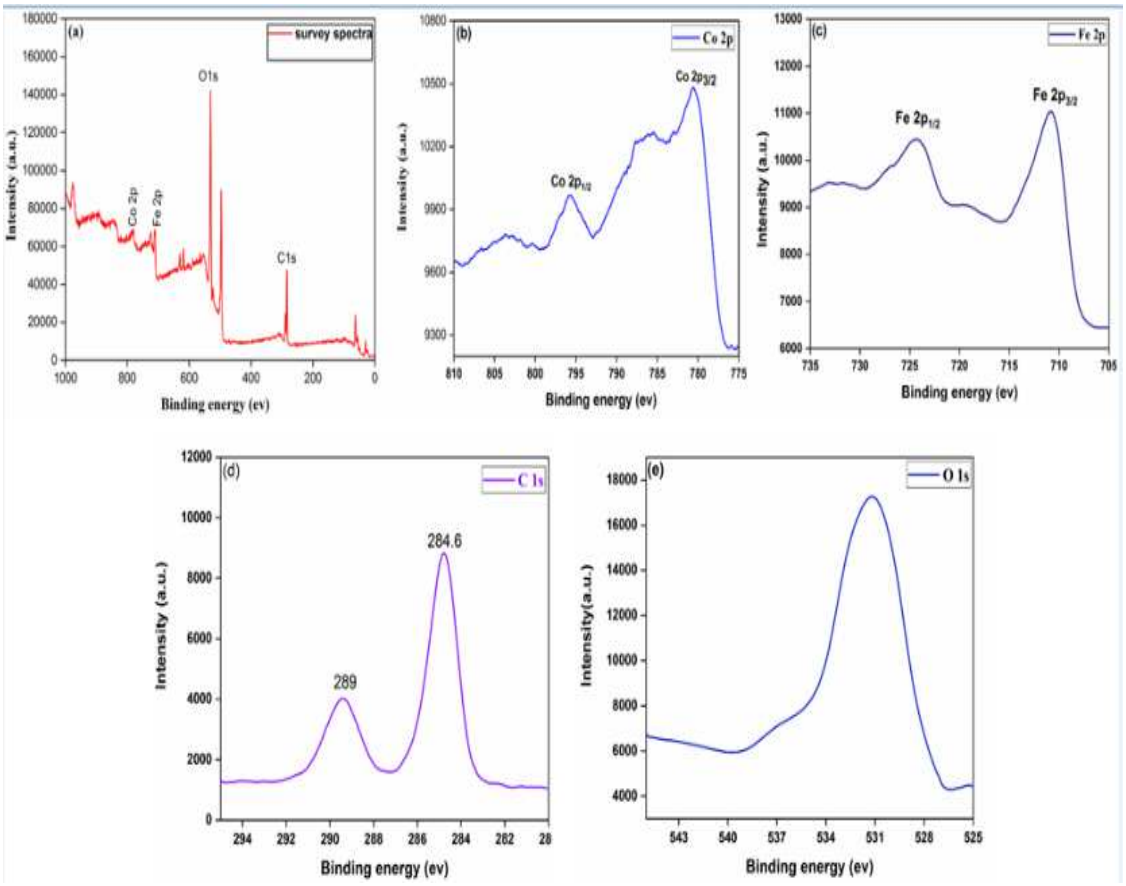


Figure 7: (a) XPS survey spectra and high-resolution spectra of (b) Co 2p, (c) Fe 2p, (d) C1s and (f) O1s for $CoFe_2O_4$@GO.

Electrochemical Measurements

The electrochemical performance of the synthesized $CoFe_2O_4$@GO nanocomposites was evaluated using a conventional three-electrode electrochemical system. The measurements were carried out using an electrochemical workstation at room temperature. The working electrode was prepared by mixing the synthesized $CoFe_2O_4$@GO nanocomposite with a suitable binder and conductive material to form a homogeneous slurry. The slurry was then coated onto a conductive substrate and allowed to dry to obtain the working electrode. A platinum wire was used as the counter electrode, while an Ag/AgCl electrode served as the reference electrode. The electrochemical measurements were performed in an appropriate 6M KOH electrolyte solution.

Cyclic Voltammetry Analysis

CV measurements were carried out to investigate and compare the electrochemical behavior of the synthesized $CoFe_2O_4$ nanoparticles and $CoFe_2O_4$@GO nanocomposites. The CV analysis was performed in a three-electrode configuration within a suitable potential window at different scan rates. The obtained CV curves exhibited distinct redox peaks, indicating that the charge storage process is mainly governed by faradaic redox reactions associated with the transition metal ions present in cobalt ferrite. It was observed that the $CoFe_2O_4$@GO nanocomposite exhibited a higher current response and larger CV curve area compared to pure $CoFe_2O_4$, indicating enhanced electrochemical activity. This improvement can be attributed to the presence of GO, which provides a larger surface area and improved electrical conductivity, facilitating faster electron transport and efficient ion diffusion during the electrochemical process. Additionally, the relatively symmetric shape of the CV curves at different scan rates suggests good reversibility of the redox reactions and favorable electrochemical kinetics. These results confirm that the incorporation of GO significantly enhances the electrochemical performance of $CoFe_2O_4$.

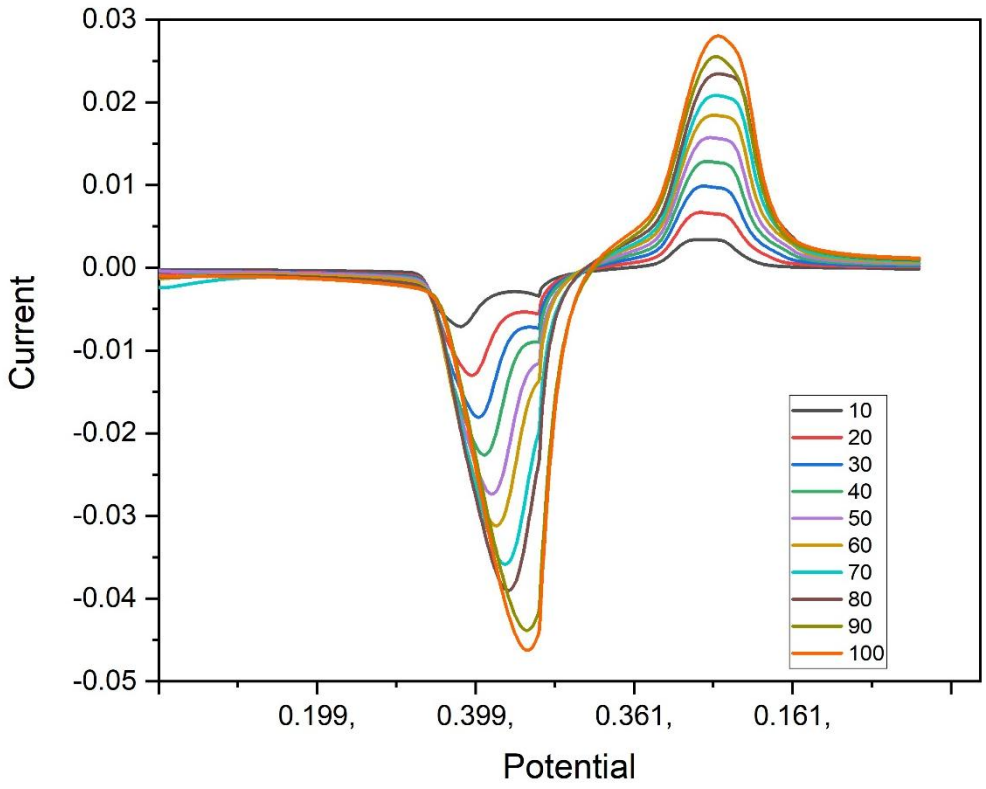


Figure 8: CV spectra of $CoFe_2O_4$.

The electrochemical kinetics of the $CoFe_2O_4$@GO electrode were further investigated by analyzing the relationship between the cathodic and anodic peak currents obtained from CV at different scan rates using the equation given below **[48].**

$$I_P = aV^b \qquad (2)$$

The peak current values were plotted against the scan rates on a logarithmic scale, and the b-value was calculated from the slope of the linear fit using the power law relationship between peak current (i) and scan rate (v). The calculated b-value provides insight into the charge storage mechanism, where a value close to 0.5 indicates diffusion-controlled behavior, while a value approaching 1.0 suggests a surface-controlled capacitive process. The obtained b-value for the $CoFe_2O_4$@GO electrode indicates that the charge storage process involves a combination of diffusion-controlled and capacitive contributions. This behavior can be attributed to the presence of graphene oxide, which enhances the surface area and electrical conductivity of the electrode, thereby facilitating efficient electron transport and ion diffusion during the electrochemical process.

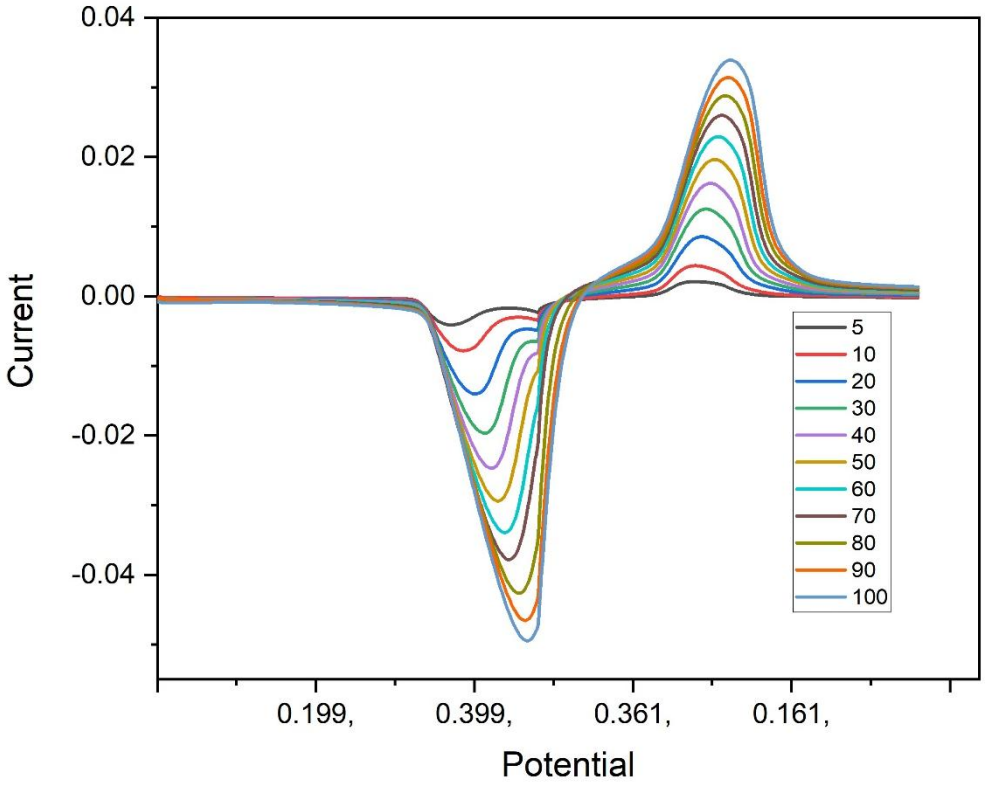


Figure 9: CV spectra of $CoFe_2O_4$@GO.

Galvanostatic Charge Discharge Analysis

GCD measurements were carried out to evaluate the electrochemical charge storage behavior of the synthesized $CoFe_2O_4$@GO nanocomposite electrode at different current densities. The obtained GCD curves exhibited nearly symmetric charge–discharge profiles, indicating good electrochemical reversibility and high coulombic efficiency of the electrode material. The relatively long discharge time observed in the GCD curves suggests a high charge storage capability and good capacitive performance of the $CoFe_2O_4$@GO electrode. This enhanced electrochemical performance can be attributed to the synergistic effect between $CoFe_2O_4$ nanoparticles and GO, where GO provides a large surface area and improved electrical conductivity, facilitating efficient electron transport and ion diffusion during the charge–discharge process. Furthermore, the consistent shape of the GCD curves at various current densities indicates good rate capability and structural stability of the $CoFe_2O_4$@GO nanocomposite, highlighting its potential application in electrochemical energy storage devices.

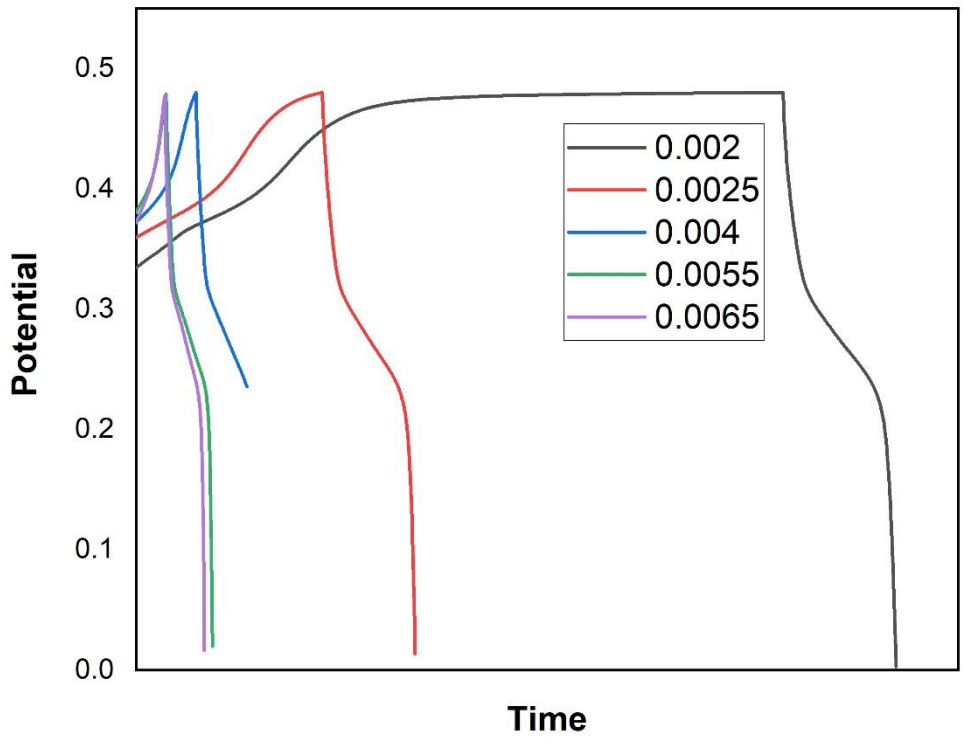


Figure 10: GCD spectra of $CoFe_2O_4$@GO.

Rate Performance

The rate performance of the $CoFe_2O_4$@GO electrode was evaluated from the GCD measurements at different current densities is shown in **Figure 11**. The specific capacitance of the electrode was calculated from the discharge curves obtained at increasing current densities. It was observed that the electrode retained a significant portion of its capacitance even at higher current densities, indicating good rate capability. This behavior can be attributed to the synergistic effect between $CoFe_2O_4$ nanoparticles and graphene oxide, where GO provides enhanced electrical conductivity and a large surface area, facilitating rapid electron transport and efficient ion diffusion within the electrode material. Furthermore, the relatively stable discharge profiles at different current densities suggest that the $CoFe_2O_4$@GO nanocomposite possesses good electrochemical stability and fast charge transfer kinetics, making it a promising electrode material for high-performance electrochemical energy storage applications.

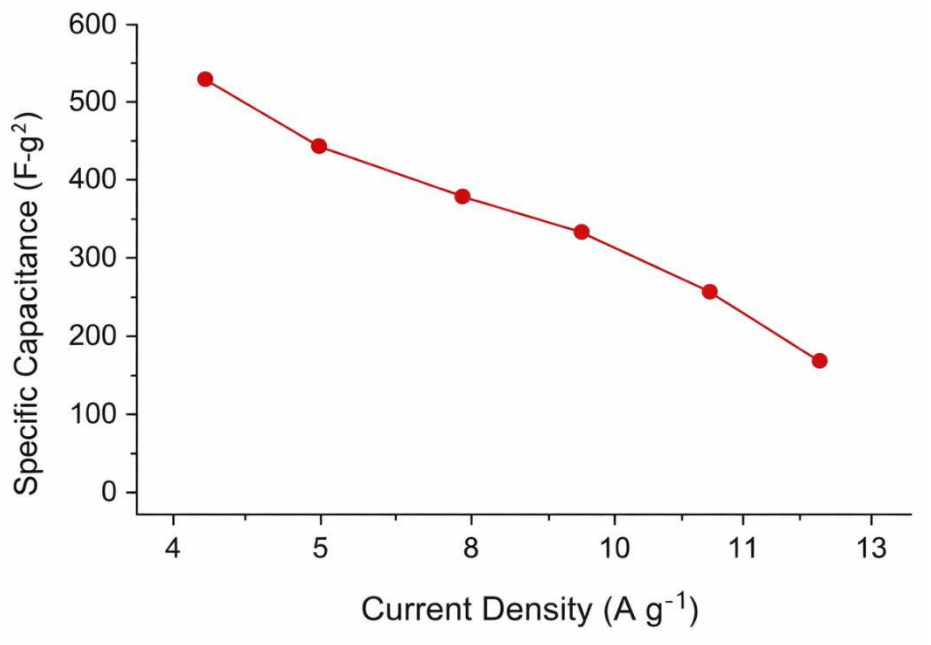


Figure 11: Rate performance of fabricated electrode.

The energy storage capability of the $CoFe_2O_4$@GO electrode was further evaluated by analyzing the relationships between energy density, power density, and current density derived from the GCD measurements according to equation 3 to equation 5 (**Table 1**) **[48].**

$$C = \frac{I*dt}{m*dV} \qquad (3)$$

$$E = \frac{CdV * dV}{2} \quad (4)$$

$$P = \frac{E}{dt} \quad (5)$$

Table 1: Depicts the Current Density, Specific Capacitance, Energy Density and Power Density.

Current (A)	**Current Density (A g^{-1})**	**Specific Capacitance (F g^{-1})**	**Energy Density (Wh kg^{-1})**	**Power Density (W kg^{-1})**	**Δt (s)**
0.002	4	541.7	17.33	959.7	65
0.0025	5	395.8	12.67	1200.6	38
0.004	8	350.0	11.20	1920	21
0.0055	11	343.8	11.00	2640	15
0.0065	13	216.7	6.93	3118.5	8

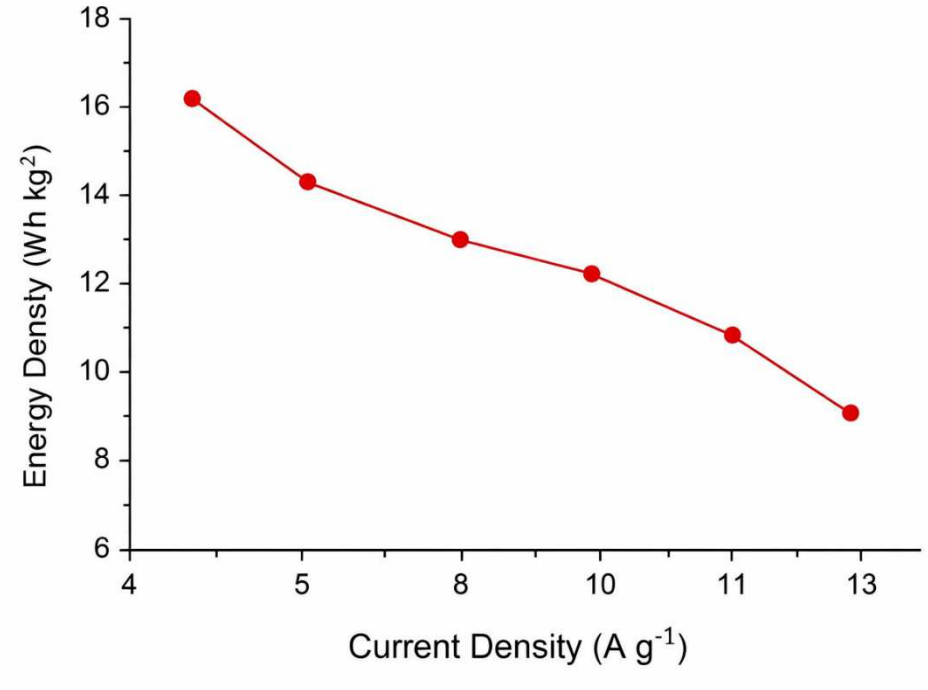


Figure 12: Plot of energy density vs current density

The energy density vs current density plot (**Figure 12**) shows that the energy density gradually decreases with increasing current density, which is mainly attributed to the reduced time available for electrolyte ions to fully diffuse into the active sites of the electrode at higher current densities. Similarly, the power density vs current density plot (**Figure 13**) demonstrates that the power density increases with increasing current density, indicating that the electrode can deliver energy rapidly under high current conditions.

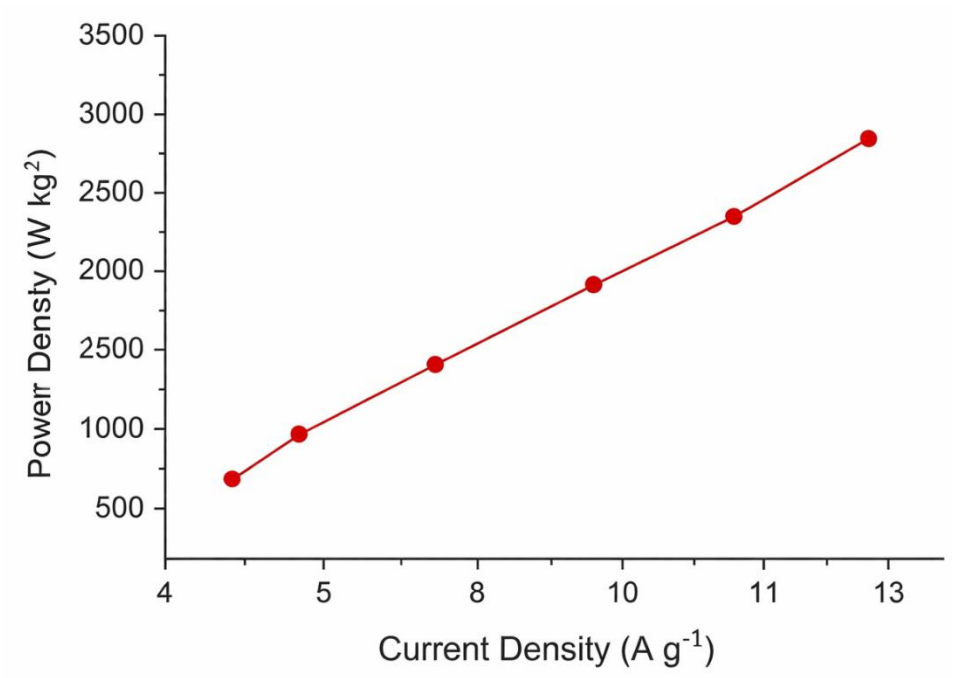


Figure 13: Plot of power density vs current density.

Furthermore, the energy density vs power density plot (**Figure 14**), commonly referred to as the Ragone plot, provides a comprehensive evaluation of the electrochemical performance of the electrode material. The Ragone plot reveals that the $CoFe_2O_4$@GO electrode maintains a relatively high energy density even at elevated power densities, highlighting its excellent balance between energy storage capability and power delivery. This improved performance can be attributed to the synergistic interaction between $CoFe_2O_4$ nanoparticles and graphene oxide, where GO enhances electrical conductivity and provides a large surface area for efficient ion transport and electron transfer. These results demonstrate that the $CoFe_2O_4$@GO nanocomposite electrode exhibits promising electrochemical properties for high-performance energy storage applications.

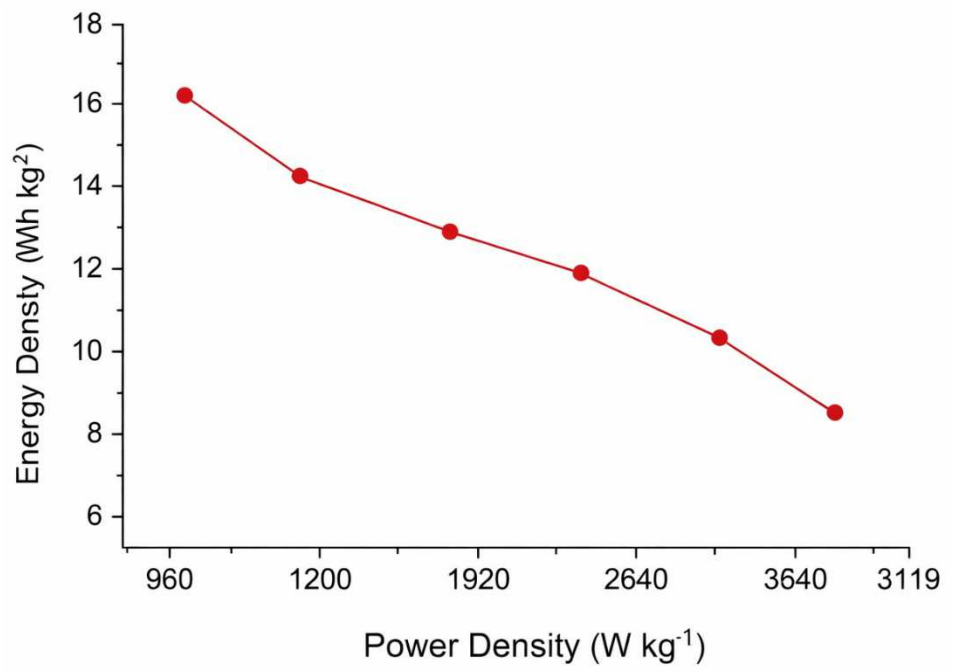


Figure 14: Plot of power density vs energy density.

Cyclic Stability

The cyclic stability (**Figure 15**) of the $CoFe_2O_4$@GO electrode was evaluated using repeated GCD measurements over a large number of charge–discharge cycles at a constant current density. The electrode exhibited stable charge–discharge profiles with minimal variation in discharge time during continuous cycling, indicating good electrochemical stability. The capacitance retention remained relatively high even after prolonged cycling, demonstrating the excellent durability of the electrode material. This improved cyclic stability can be attributed to the strong interaction between $CoFe_2O_4$ nanoparticles and GO sheets, where GO acts as a conductive matrix that enhances electrical conductivity and buffers the structural changes occurring during repeated charge–discharge processes. Furthermore, the robust structure of the $CoFe_2O_4$@GO nanocomposite helps maintain efficient electron transport and ion diffusion throughout the cycling process. These results indicate that the $CoFe_2O_4$@GO electrode possesses good long-term electrochemical stability, making it a promising candidate for energy storage applications such as supercapacitors.

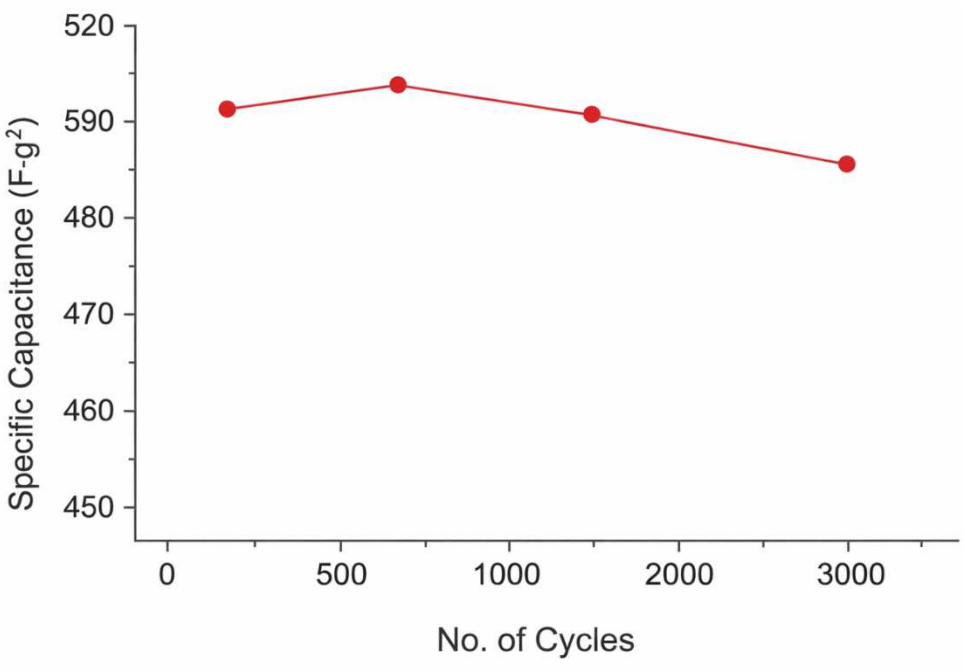


Figure 15: Cyclic stability.

EIS Analysis

EIS was performed to investigate the charge transfer resistance and ion transport properties of the $CoFe_2O_4$@GO electrode. The EIS measurements were carried out over a wide frequency range to analyze the electrochemical kinetics of the electrode material. The obtained Nyquist plot (**Figure 16**) typically consists of a straight line in the low-frequency region. The straight line in the low-frequency region is associated with the Warburg impedance, which represents the diffusion of electrolyte ions into the electrode material. The relatively small semicircle diameter in the Nyquist plot indicates low charge transfer resistance, suggesting efficient electron transport within the $CoFe_2O_4$@GO nanocomposite. This improved conductivity can be attributed to the presence of graphene oxide, which provides a conductive network and facilitates rapid electron movement during the electrochemical process. Additionally, the nearly vertical line in the low-frequency region reflects good capacitive behavior and efficient ion diffusion within the electrode structure. These results demonstrate that the $CoFe_2O_4$@GO electrode exhibits favorable electrochemical kinetics and low internal resistance, which contribute to its enhanced electrochemical performance in energy storage applications.

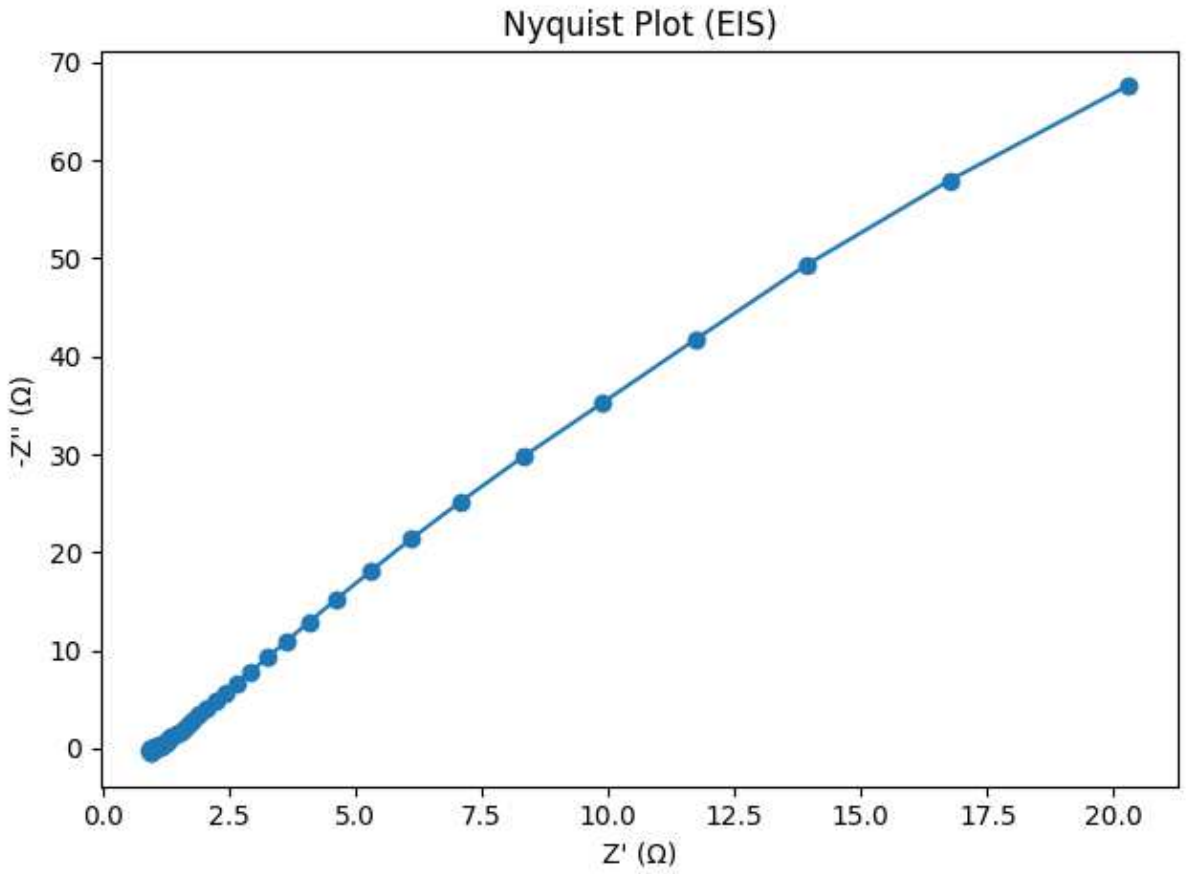


Figure 16: Nyquist plot.

Conclusion

In summary, $CoFe_2O_4$ nanoparticles and $CoFe_2O_4$@GO nanocomposites were successfully synthesized through a facile co-precipitation method and evaluated as electrode materials for supercapacitor applications. Structural and chemical characterization using XRD, FESEM, FTIR and XPS confirmed the successful formation of cobalt ferrite and its effective integration with graphene oxide. The electrochemical studies carried out using CV, GCD and EIS techniques demonstrated that the incorporation of graphene oxide significantly enhances the electrochemical performance of cobalt ferrite. The $CoFe_2O_4$@GO electrode exhibited higher current response, improved charge–discharge behavior, better rate capability, and lower charge transfer resistance compared to pure $CoFe_2O_4$. These improvements can be attributed to the synergistic interaction between cobalt ferrite nanoparticles and graphene oxide, where GO provides a conductive network, larger surface area, and facilitates faster electron transport and ion diffusion during the electrochemical process. In addition, the $CoFe_2O_4$@GO electrode showed good cyclic stability, indicating its structural robustness during repeated charge–discharge cycles. Overall, the results demonstrate that $CoFe_2O_4$@GO

nanocomposites are promising electrode materials for advanced electrochemical energy storage devices, particularly for high-performance supercapacitor applications.

Declaration of Competing Interest

The authors have no relevant financial or non-financial interests to disclose.

Data Availability Statement

The data that support the findings of this study are available from the corresponding author upon reasonable request.

Funding

There is no funding source for this work.

References

[1] Habib, A. and Sou, C., 2018. Analytical review on the trends and present situation of large-scale sustainable energy storage technology. European Journal of Sustainable Development Research, 2(3), p.31.

[2] Audu, G.A., Mafo, A.R., Jegede, R.E., Tarasenko, M. and Kozak, K., 2025. Advances in energy storage technologies for renewable energy systems: bridging intermittency and sustainable integration. Eurasian Journal of Physics and Functional Materials, 9(2).

[3] Guo, J., Jing, Y., Hou, W., Wang, T., Ma, S. and He, G., 2024. Demands and challenges of energy storage technology for future power system. Energy Internet, 1(2), pp.116-122.

[4] Saleh, H.M. and Hassan, A.I., 2024. The challenges of sustainable energy transition: A focus on renewable energy. Applied Chemical Engineering, 7(2), p.2084.

[5] Al-Ghaili, A.M., Kasim, H., Aris, H. and Al-Hada, N.M., 2022. Can electric vehicles be an alternative for traditional fossil-fuel cars with the help of renewable energy sources towards energy sustainability achievement?. Energy Informatics, 5(Suppl 4), p.60.

[6] Cherwoo, L., Gupta, I., Flora, G., Verma, R., Kapil, M., Arya, S.K., Ravindran, B., Khoo, K.S., Bhatia, S.K., Chang, S.W. and Ngamcharussrivichai, C., 2023. Biofuels an alternative to traditional fossil fuels: A comprehensive review. Sustainable Energy Technologies and Assessments, 60, p.103503.

[7] Olabi, A.G., Abbas, Q., Al Makky, A. and Abdelkareem, M.A., 2022. Supercapacitors as next generation energy storage devices: Properties and applications. Energy, 248, p.123617.

[8] Czagany, M., Hompoth, S., Keshri, A.K., Pandit, N., Galambos, I., Gacsi, Z. and Baumli, P., 2024. Supercapacitors: An efficient way for energy storage application. Materials, 17(3), p.702.

[9] Ramachandran, T., Sana, S.S., Kumar, K.D., Kumar, Y.A., Hegazy, H.H. and Kim, S.C., 2023. Asymmetric supercapacitors: Unlocking the energy storage revolution. Journal of Energy Storage, 73, p.109096.

[10] Ates, M., Chebil, A., Yoruk, O., Dridi, C. and Turkyilmaz, M., 2022. Reliability of electrode materials for supercapacitors and batteries in energy storage applications: a review. Ionics, 28(1), pp.27-52.

[11] Ahsan, M.B.F., Mekhilef, S., Soon, T.K., Mubin, M.B., Shrivastava, P. and Seyedmahmoudian, M., 2022. Lithium-ion battery and supercapacitor-based hybrid energy storage system for electric vehicle applications: a review. International Journal of Energy Research, 46(14), pp.19826-19854.

[12] Ashritha, M.G. and Hareesh, K., 2023. Electrode materials for EDLC and pseudocapacitors. In Smart Supercapacitors (pp. 179-198). Elsevier.

[13] Khot, M. and Kiani, A., 2022. A review on the advances in electrochemical capacitive charge storage in transition metal oxide electrodes for pseudocapacitors. International Journal of Energy Research, 46(15), pp.21757-21796.

[14] Gharahcheshmeh, M.H. and Chowdhury, K., 2024. Fabrication methods, pseudocapacitance characteristics, and integration of conjugated conducting polymers in electrochemical energy storage devices. Energy Advances, 3(11), pp.2668-2703.

[15] Sahoo, S., Kumar, R., Joanni, E., Singh, R.K. and Shim, J.J., 2022. Advances in pseudocapacitive and battery-like electrode materials for high performance supercapacitors. Journal of Materials Chemistry A, 10(25), pp.13190-13240.

[16] Kumar, A., Rathore, H.K., Sarkar, D. and Shukla, A., 2022. Nanoarchitectured transition metal oxides and their composites for supercapacitors. Electrochemical Science Advances, 2(6), p.e2100187.

[17] Divya, T., Sarankumar, R., Balamurugan, K.S., Sakthivel, P. and Sivakami, A.J.J.O.N.R., 2025. Recent advances in transition metal oxide composites for enhanced supercapacitor performance: a comprehensive overview. Journal of Nanoparticle Research, 27(2), p.55.

[18] Al Kiey, S.A., Ahmad, M.M. and Azab, A.A., 2026. Tailoring cobalt-doped nickel ferrite nanostructures for high-performance supercapacitors. Journal of Energy Storage, 148, p.119968.

[19] Jain, P., Ansari, M.R., Peta, K.R., Thakur, O.P. and Sanger, A., 2025. Exploring advanced $CoFe_2O_4$/NiO nanocomposites with tunable structural, electrical, and

magnetic properties for electrochemical energy storage. Materials Science and Engineering: B, 321, p.118522.

[20] Chang, J.H., Prakash, N., Narendhar, C., Shen, S.Y., Govindaraju, S., Yun, K., Kumar, M. and Shkir, M., 2024. Ferrite nanomaterials for energy storage applications. In Materials for Energy Storage (pp. 126-142). CRC Press.

[21] Salama, R.S., Alshammari, R.H., Nafady, A., Soomro, R.A., Gouda, M.S. and Awad, F.S., 2024. The role of cobalt ferrites nanoparticles on structural and electrochemical properties of mesoporous silica for supercapacitor applications. Journal of Inorganic and Organometallic Polymers and Materials, 34(6), pp.2418-2431.

[22] Ansari, S.M., Younis, A., Kolekar, Y.D. and Ramana, C.V., 2025. Cobalt ferrite nanoparticles: The physics, synthesis, properties, and applications. Applied Physics Reviews, 12(2).

[23] Thakur, P., Gahlawat, N., Punia, P., Kharbanda, S., Ravelo, B. and Thakur, A., 2022. Cobalt nanoferrites: a review on synthesis, characterization, and applications. Journal of Superconductivity and Novel Magnetism, 35(10), pp.2639-2669.

[24] Sukoviene, A., Ali, S., Jagminas, A. and Ramanavicius, S., 2025. Magnetic cobalt and other types of ferrite nanoparticles: synthesis aspects and novel strategies for application in wastewater treatment. Applied Sciences, 15(2), p.857.

[25] Majumder, P. and Gangopadhyay, R., 2022. Evolution of graphene oxide (GO)-based nanohybrid materials with diverse compositions: an overview. RSC advances, 12(9), pp.5686-5719.

[26] Wu, J., Lin, H., Moss, D.J., Loh, K.P. and Jia, B., 2023. Graphene oxide for photonics, electronics and optoelectronics. Nature Reviews Chemistry, 7(3), pp.162-183.

[27] Ghulam, A.N., Dos Santos, O.A., Hazeem, L., Pizzorno Backx, B., Bououdina, M. and Bellucci, S., 2022. Graphene oxide (GO) materials—applications and toxicity on living organisms and environment. Journal of Functional Biomaterials, 13(2), p.77.

[28] Razaq, A., Bibi, F., Zheng, X., Papadakis, R., Jafri, S.H.M. and Li, H., 2022. Review on graphene-, graphene oxide-, reduced graphene oxide-based flexible composites: from fabrication to applications. Materials, 15(3), p.1012.

[29] Priyadharshini, A., Vinodhini, S.P. and Xavier, J.R., 2026. A comprehensive review of graphene-based nanocomposites for high-performance energy storage: advances in design, electrochemical mechanisms, and future prospects. Ionics, pp.1-38.

[30] Osman, A., Elhakeem, A., Kaytbay, S. and Ahmed, A., 2022. A comprehensive review on the thermal, electrical, and mechanical properties of graphene-based multi-functional epoxy composites. Advanced Composites and Hybrid Materials, 5(2), pp.547-605.

[31] Thakur, P., Gahlawat, N., Punia, P., Kharbanda, S., Ravelo, B. and Thakur, A., 2022. Cobalt nanoferrites: a review on synthesis, characterization, and applications. Journal of Superconductivity and Novel Magnetism, 35(10), pp.2639-2669.

[32] Kashid, P., Suresh, H.K., Mathad, S.N., Shedam, R. and Shedam, M., 2022. A review on synthesis, properties and applications on cobalt ferrite. Int. J. Adv. Sci. Eng, 9, pp.2567-2583.

[33] Krishnan, Y., Babu, K., Sakkaraiyan, S., Dinesh, A., Shanmugam, A., Radhakrishnan, K. and Ayyar, M., 2024. Spinel cobalt ferrite nanoparticles for photocatalysts, sensor and biomedical applications: a review. Semiconductors, 58(9), pp.721-739.

[34] Khan, M.M., 2025. Precipitation and coprecipitation synthesis methods. Photocatalysts: synthesis and characterization methods, pp.11-25.

[35] Alzaid, M., Abu-Dief, A.M., Hadia, N.M.A., Ezzeldien, M. and Mohamed, W.S., 2024. Synthesis and characterization study of spinel Co_3O_4 nanoparticles synthesized via the facial co-precipitation route for optoelectronic application. Optical and Quantum Electronics, 56(7), p.1156.

[36] Matteppanavar, S., Manjanna, J. and Hegde, B.G., 2023. Structural, electrical and magnetic properties of Pr doped $Co_{0.5}Zn_{0.5}Fe_2O_4$ nanoparticles. Materials Today: Proceedings, 82, pp.390-394.

[37] Basak, M., Rahman, M.L., Ahmed, M.F., Biswas, B. and Sharmin, N., 2022. The use of X-ray diffraction peak profile analysis to determine the structural parameters of cobalt ferrite nanoparticles using Debye-Scherrer, Williamson-Hall, Halder-Wagner and Size-strain plot: Different precipitating agent approach. Journal of Alloys and Compounds, 895, p.162694.

[38] Dubey, K., Dubey, S., Sahu, V., Modi, A., Bamne, J., Haque, F.Z. and Gaur, N.K., 2023. Defects and oxygen vacancies modified properties of transition metal doped $Ce_{0.95}X_{0.05}O_2$ (X= Fe, Co, Ni) nanoparticles. Materials Science and Engineering: B, 288, p.116154.

[40] Shanmugapriya, I.G., Sa, S. and Natarajan, S., 2025. Synthesis, structure, oxygen evolution reaction (OER) and visible-light assisted organic reaction studies on A 2 M 2 TeB 2 O 10 (A= Ba and Pb; M= Mg, Zn, Co, Ni, Cu, and Fe). Dalton Transactions, 54(7), pp.2753-2764.

[41] Yusuf, M.O., 2023. Bond characterization in cementitious material binders using Fourier-transform infrared spectroscopy. Applied Sciences, 13(5), p.3353.

[42] Song, J., Kim, S. and Kim, J., 2025. Enhancing antibody capture with edge-carboxyl-enriched, low-defect monolayer graphene oxide via controlled graphite oxidation. Carbon, p.121115.

[43] Huo, D., Li, X., Yu, B., Chen, J., Dong, J., Liu, J. and Nan, D., 2025. Enhancing mechanical properties of epoxy resin composites with aluminum oxide-modified graphene oxide. Diamond and Related Materials, 151, p.111864.

[44] Greczynski, G., Haasch, R.T., Hellgren, N., Lewin, E. and Hultman, L., 2023. X-ray photoelectron spectroscopy of thin films. Nature Reviews Methods Primers, 3(1), p.40.

[45] Ansari, S.M., Phase, D., Kolekar, Y.D. and Ramana, C.V., 2024. Effect of Manganese-Doping on the chemical and optical properties of cobalt ferrite nanoparticles. Materials Science and Engineering: B, 300, p.117134.

[46] Gupta, A. and Sahni, M., 2024. Structural and magnetic properties of cobalt ferrite nano-particles. Materials Today: Proceedings, 104, pp.11-21.

[47] Ansari, S.M., Sinha, B.B., Sen, D., Sastry, P.U., Kolekar, Y.D. and Ramana, C.V., 2022. Effect of oleylamine on the surface chemistry, morphology, electronic structure, and magnetic properties of cobalt ferrite nanoparticles. Nanomaterials, 12(17), p.3015.

[48] Sharma, M., Ahmed, A., Singh, A., Jamwal, P. and Arya, S., 2025. Combustion synthesis, spectral and electrochemical characterization of chromium-doped magnesium ferrite ($MgFe_2O_4$) nanoparticles for enhanced supercapacitor electrode performance. Inorganic Chemistry Communications, 180, p.114912.